Computer Assisted Mechanics and Engineering Sciences, 3: 403–423, 1996.

A sensitivity analysis for frictionless contact problems

Xian Chen and Masahiko Mori
Takasago R&D Center, Mitsubishi Heavy Industries, LTD.
2-1-1, Shinhama Arai-Cho, Takasago, Hyogo Pref. 676, Japan

Toshiaki Hisada
Department of Mechano-Informatics, The University of Tokyo
7-3-1 Hongo, Bunkyo-Ku, Tokyo, 113, Japan

(Received July 29, 1996)

A sensitivity analysis method for elasto-plastic contact problems with large deformation is developed based on two contact constraint methods, i.e., the Lagrange multiplier and penalty methods. Throughout the formulation the importance of using consistent contact stiffness in the sensitivity analysis is emphasized, and is demonstrated in a simple contact problem. Also a heat-transfer tube and plate contact system of heat exchanger used in PWR is analyzed as a real numerical example. The obtained sensitivities of residual stress resulting from the tube expansion process are discussed so as to provide implications for design improvement and quality control.

1. Introduction

In advanced engineering applications, both the response of the system and its rate with respect to a particular system parameter are often used. Over the years sensitivity analysis methods have been developed to compute this rate. These methods were initially applied to several engineering fields, including structural optimization problems [18], and have subsequently been used in other fields, e.g., reliability and statistical structural analyses [1, 7, 10].

Sensitivity analysis methods in nonlinear finite element structural analysis can be categorized into three classes: the finite difference method, the direct differentiation method and the adjoint variable method. The first method is the easiest to implement and has been widely employed. However, its computational efficiency is poor, especially for nonlinear problems, because iterative computation must be repeated as many as the number of design variables. On the other hand, in the direct differentiation method the equilibrium equation or its performance functional is directly differentiated to obtain the derivative of structural response with respect to a design variable. In this approach, nonlinear analysis, which consumes large amount of CPU time, is required only for the original system and not for the sensitivity analysis; hence high computational efficiency is achieved. In the adjoint variable method, which has been extensively used in optimal control theory (see, e.g., [4, 5]), by solving an adjoint structure equation after analyzing the original system, the response sensitivity can be directly obtained without calculating the displacement sensitivity. The adjoint variable method is particularly efficient for cases in which the number of design variables is large relative to the number of response sensitivities which one wishes to know, whereas it becomes cumbersome for path-dependent problems. Sensitivity analysis methods for path-dependent problems have been studied in [2, 8, 13, 14, 15], and will not be discussed here.

Recently, engineering application research has been successfully carried out on the contact problems with large deformation (see [17] as a review). The development of a sensitivity analysis method for this particularly complex system seems to be important because it will help engineer to have an insight into the problem. Kleiber [9] has proposed a sensitivity analysis procedure

for two-dimensional unilateral frictional contact problems, where frictional traction is treated with Coulomb's law and the direct differentiation method is used for sensitivity analysis. Considering the nature of contact problems, consistent formulation must be made in the sensitivity analysis algorithm for treating boundary conditions and introducing contact constraints exerted on the contact boundaries. Moreover, inelasticity, when introduced, should be suitably involved in the sensitivity analysis formulation. As seen in elasto-plastic problems, the use of consistent (strict) tangent stiffness in the sensitivity analysis formulation is indispensable. This point will be emphasized and exemplified in this paper.

In the next section, computational procedures for frictionless contact problems with elasto-plasticity and large deformation will be summarized, where two contact constraint methods, i.e., the Lagrange multiplier and penalty methods are introduced. In Section 3, sensitivity analysis algorithms based on these methods are formulated. It is supposed that these algorithms can also be applied for other constraint methods. In Section 4, the proposed numerical procedures are applied to a couple of numerical examples including a real engineering problem.

2. Finite element formulation for frictionless contact problems

In this section, the finite element formulation for frictionless contact problems is outlined based on the works [11] and [16], and the consistent tangent stiffness is newly introduced for use in the sensitivity analysis which will be given in the next section.

For a frictionless contact problem, the virtual work done at time t in the contact area of two bodies, indicated with right superscripts 1 and 2, is defined by

$$\delta\, {}^{t}W_{\mathrm{c}} = \int_{{}^{t}\Gamma_{\mathrm{c}}^{1}} {}^{t}\mathbf{p}_{\mathrm{n}}^{1} \cdot \delta\, {}^{t}\mathbf{u}^{1}\, \mathrm{d}s + \int_{{}^{t}\Gamma_{\mathrm{c}}^{2}} {}^{t}\mathbf{p}_{\mathrm{n}}^{2} \cdot \delta\, {}^{t}\mathbf{u}^{2}\, \mathrm{d}s\,, \tag{1}$$

where

$${}^{t}\mathbf{p}_{\mathrm{n}}^{i} = ({}^{t}\mathbf{p}_{\mathrm{n}}^{i} \cdot {}^{t}\mathbf{n}^{i})\, {}^{t}\mathbf{n}^{i} = {}^{t}p_{\mathrm{n}}^{i}\, {}^{t}\mathbf{n}^{i}\,, \tag{2}$$

$${}^{t}\Gamma_{\mathrm{c}}^{1} = {}^{t}\Gamma_{\mathrm{c}}^{2}\,. \tag{3}$$

${}^{t}\mathbf{p}_{\mathrm{n}}^{i}$ and ${}^{t}\mathbf{n}^{i}$ represent the contact traction and normal vector on the contact surface of body i, respectively. ${}^{t}\Gamma_{\mathrm{c}}^{i}$ denotes the contact area of body i. Clearly,

$${}^{t}\mathbf{p}_{\mathrm{n}}^{1} = -{}^{t}\mathbf{p}_{\mathrm{n}}^{2}\,. \tag{4}$$

Substituting Eq. (4) into Eq. (1) leads to

$$\delta\, {}^{t}W_{\mathrm{c}} = \int_{{}^{t}\Gamma_{\mathrm{c}}^{1}} {}^{t}\mathbf{p}_{\mathrm{n}}^{1} \cdot (\delta\, {}^{t}\mathbf{u}^{1} - \delta\, {}^{t}\mathbf{u}^{2})\, \mathrm{d}s\,. \tag{5}$$

On the other hand, the penetration can be defined as

$${}^{t}g = ({}^{t}\mathbf{x}^{2} - {}^{t}\mathbf{x}^{1}) \cdot {}^{t}\mathbf{n}^{1}\,, \tag{6}$$

where ${}^{t}\mathbf{x}^{1}$ and ${}^{t}\mathbf{x}^{2}$ are the position vectors on the contact surfaces, and the contact constraint becomes

$${}^{t}g \geq 0\,. \tag{7}$$

Noting that the traction must be compressive for contacting bodies and zero when two bodies separate, we have a standard relation in the so-called Kuhn–Tucker form

$${}^{t}g \geq 0\,, \quad {}^{t}p_{\mathrm{n}}^{1} \leq 0\,, \quad {}^{t}g \cdot {}^{t}p_{\mathrm{n}}^{1} = 0\,. \tag{8}$$

Incorporating the internal virtual work and the virtual work of applied load and contact traction for bodies 1 and 2 gives

$$\int_v \mathbf{T} : (\delta\mathbf{u} \otimes \nabla_{\mathbf{x}})\, dv = \int_{s_t} \underline{\mathbf{t}} \cdot \delta\mathbf{u}\, ds + \int_v \rho\mathbf{g} \cdot \delta\mathbf{u}\, dv + \int_{{}^t\Gamma_c^1} {}^t p_n^1\, {}^t\mathbf{n}^1 \cdot \left(\delta\, {}^t\mathbf{u}^1 - \delta\, {}^t\mathbf{u}^2\right) ds\,. \tag{9a}$$

The nonpenetration condition in the contact area is expressed in weak form as

$$\int_{{}^t\Gamma_c^1} \delta\, {}^t p_n^1\, {}^t g\, ds = 0\,. \tag{9b}$$

Taking contact force ${}^t p_n^1$ as an independent variable yields the Lagrange multiplier method. Equations (9a) and (9b) are solved simultaneously. On the other hand, in the penalty method, contact force ${}^t p_n^1$ is treated as a function of penetration and hence as a function of displacement. In this case, only Eq. (9a) is solved and the contact force can be evaluated from the displacement field.

The weak forms (9a) and (9b) have clear physical meanings and are independent of the material models used for contacting bodies. Due to the *a priori* unknown contact boundary, a trial-and-error procedure is usually used to solve contact problems, especially when large deformation occurs.

A discretization model for a potential contact surface is shown in Fig. 1.

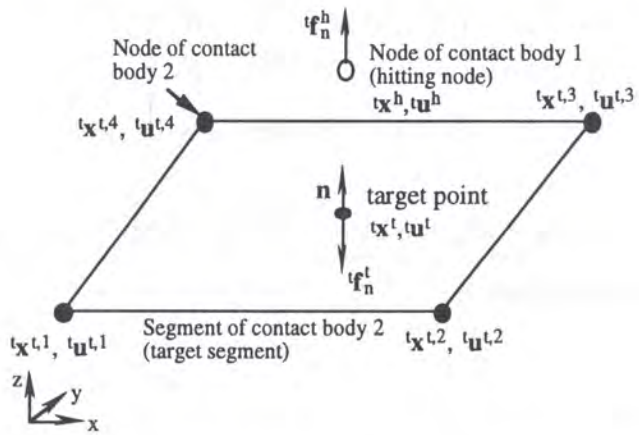

Fig. 1. A node-to-segment contact model

Contact surfaces are classified into two parts, called the slave and master parts. The contact node in the slave part is referred to as the hitting node, while in the master part the contact segment is called the target segment. When no hitting node is allowed to penetrate a target segment, while any segment spanned by hitting nodes is allowed to be penetrated by a node belonging to any target segment, this is called the one-pass approach. In the two-pass approach, no segment of any contact surface can be penetrated [16]. Although only one-pass approach is considered here, the presented procedure can be directly applied to two-pass approach by inversely defining the hitting node and target segment and carrying out the procedure again.

Let us consider a pair of hitting node and target segment, as shown in Fig. 1, which are assumed to be in contact. The target point, namely, the contact point in the target segment, is defined as the closest point to the hitting node, and the target point ${}^t\mathbf{x}^{\mathrm{t}}$, hitting node ${}^t\mathbf{x}^{\mathrm{h}}$, and normal unit vector ${}^t\mathbf{n}$ of the target segment at the target point can be related to the amount of penetration of the hitting node, i.e., ${}^t g$, by

$${}^t g = \left({}^t\mathbf{x}^{\mathrm{t}} - {}^t\mathbf{x}^{\mathrm{h}}\right) \cdot {}^t\mathbf{n}\,, \tag{10}$$

where the right superscripts t and h respectively denote the target point and hitting node, and the left superscript t denotes instantaneous time t. By transforming the contact traction into the discrete nodal contact force, the discretized form of virtual work $\delta\, {}^t w_c$ at time t can be similarly obtained as Eq. (1) using ${}^t\mathbf{f}_n^{\mathrm{t}} = -{}^t\mathbf{f}_n^{\mathrm{h}}$, i.e.,

$$\begin{aligned}\delta^t w_c &= {}^t\mathbf{f}_n^t \cdot \delta^t\mathbf{u}^t + {}^t\mathbf{f}_n^h \cdot \delta^t\mathbf{u}^h \\ &= {}^t\mathbf{f}_n^t \cdot \left(\delta^t\mathbf{u}^t - \delta^t\mathbf{u}^h\right) \\ &= {}^tf_n^t\,{}^t\mathbf{n} \cdot \left(\delta^t\mathbf{u}^t - \delta^t\mathbf{u}^h\right), \end{aligned} \tag{11}$$

where ${}^t\mathbf{f}_n^h$ and ${}^t\mathbf{f}_n^t$ are the contact forces acting on the hitting node and target point. Displacement of the target point can be interpolated by nodal displacements of the target segment with shape functions

$$\delta\,{}^t\mathbf{u}^t = \sum_{i=1}^{m} N_i\,\delta\,{}^t\mathbf{u}^{t,i}. \tag{12}$$

Therefore, in matrix form,

$$\delta\,{}^t\mathbf{u}^t - \delta\,{}^t\mathbf{u}^h = \mathbf{M}\,\delta\,{}^t\mathbf{u}_c, \tag{13}$$

where

$$\mathbf{M} = \begin{bmatrix} -1 & 0 & 0 & N_1 & 0 & 0 & \dots & N_m & 0 & 0 \\ 0 & -1 & 0 & 0 & N_1 0 & & \dots & 0 & N_m & 0 \\ 0 & 0 & -1 & 0 & 0 & N_1 & \dots & 0 & 0 & N_m \end{bmatrix} \tag{14}$$

and

$$\delta\,{}^t\mathbf{u}_c^{\mathrm{T}} = \left\{\delta\,{}^tu_1^h\ \delta\,{}^tu_2^h\ \delta\,{}^tu_3^h\ \delta\,{}^tu_1^{t,1}\ \delta\,{}^tu_2^{t,1}\ \delta\,{}^tu_3^{t,1}\ \dots\ \delta\,{}^tu_1^{t,m}\ \delta\,{}^tu_2^{t,m}\ \delta\,{}^tu_3^{t,m}\right\}. \tag{15}$$

Representing the normal unit vector as

$${}^t\mathbf{n} = \{{}^tn_1\ {}^tn_2\ {}^tn_3\}^{\mathrm{T}} \tag{16}$$

and considering Eq. (11) gives

$$\delta^t w_c = \delta\,{}^t\mathbf{u}_c^{\mathrm{T}}\,\mathbf{M}^{\mathrm{T}}\,{}^t\mathbf{n}\ {}^tf_n^t = \delta\,{}^t\mathbf{u}_c^{\mathrm{T}}\,{}^t\mathbf{f}_c, \tag{17}$$

where ${}^t\mathbf{f}_c$ is the equivalent contact nodal force vector of the hitting node and the nodes surrounding the target segment. On the other hand, using the isoparametric formulation similarly to Eq. (13), the matrix form of Eq. (10) can be given as

$${}^tg = {}^t\mathbf{n}^{\mathrm{T}}\,\mathbf{M}\,{}^t\mathbf{x}_c \tag{18}$$

where

$${}^t\mathbf{x}_c^{\mathrm{T}} = \left\{{}^tx_1^h\ {}^tx_2^h\ {}^tx_3^h\ {}^tx_1^{t,1}\ {}^tx_2^{t,1}\ {}^tx_3^{t,1}\ \dots\ {}^tx_1^{t,m}\ {}^tx_2^{t,m}\ {}^tx_3^{t,m}\right\}. \tag{19}$$

The contact constraint condition gives

$${}^tg = 0. \tag{20}$$

By assembling ${}^t\mathbf{f}_c$ and ${}^tg$ for L hitting nodes, the total contact nodal force ${}^t\mathbf{F}_c$ and penetration for the whole contact system can be expressed as

$${}^t\mathbf{F}_c = \mathop{\mathsf{A}}_{i=1}^{L} \left[{}^t\mathbf{f}_c\right]_i, \tag{21}$$

$${}^t\mathbf{G} = \mathop{\mathsf{A}}_{i=1}^{L} \left[{}^tg\right]_i. \tag{22}$$

Then the equilibrium equation of the contact system can be obtained from Eqs. (9a), (9b) as

$$^{t}\mathbf{Q} = {}^{t}\mathbf{F} + {}^{t}\mathbf{F}_{\mathrm{c}}\,, \tag{23}$$

where $^{t}\mathbf{Q}$ and $^{t}\mathbf{F}$ denote the nodal internal force and applied load respectively.

To satisfy the kinematic contact condition, there are two basic contact constraint methods, i.e., the Lagrange multiplier and the penalty methods. In the former, the contact force is taken as a new variable and the kinematic contact condition is exactly satisfied. In the latter, no extra variable is introduced but minute penetration is allowed. In addition to these two approaches, several other constraint methods have been proposed to improve the computational performance, e.g., the perturbed [12] and augmented [6] Lagrangian methods.

The normal vector significantly changes due to the deformation of contact bodies in large-deformation problems. Consequently, to construct a contact tangent stiffness which is consistent with the deformation of contact bodies, it is necessary to take into account the change in the normal vector since it affects the stability and convergence rate of the computation [11, 16]. For this purpose, consistent contact tangent stiffness is introduced below in accordance with each contact constraint method employed.

Equivalent nodal contact force is obtained from Eq. (17) as

$$^{t}\mathbf{f}_{\mathrm{c}} = \mathbf{M}^{\mathrm{T}}\, {}^{t}\mathbf{n}\, {}^{t}f_{\mathrm{n}}^{\mathrm{t}}\,. \tag{24}$$

Differentiation with respect to displacement gives

$$\mathrm{d}^{t}\mathbf{f}_{\mathrm{c}} = \mathrm{d}^{t}f_{\mathrm{n}}^{\mathrm{t}}\, \mathbf{M}^{\mathrm{T}}\, {}^{t}\mathbf{n} + \mathrm{d}\mathbf{M}^{\mathrm{T}}\, {}^{t}\mathbf{n}\, {}^{t}f_{\mathrm{n}}^{\mathrm{t}} + \mathbf{M}^{\mathrm{T}}\, \mathrm{d}^{t}\mathbf{n}\, {}^{t}f_{\mathrm{n}}^{\mathrm{t}}\,. \tag{25}$$

Using the relations (14) and (16) and considering that the local coordinate and normal vector at the target point depend upon nodal displacement, differentiation of the equivalent contact nodal force can be obtained as

$$\mathrm{d}^{t}\mathbf{f}_{\mathrm{c}} = \mathrm{d}^{t}f_{\mathrm{n}}^{\mathrm{t}}\, \mathbf{M}^{\mathrm{T}}\, {}^{t}\mathbf{n} + (\mathbf{k}_{\mathrm{c1}} + \mathbf{k}_{\mathrm{c2}})\mathrm{d}\mathbf{u}_{\mathrm{c}}\,, \tag{26}$$

where $\mathbf{k}_{\mathrm{c1}}$ and $\mathbf{k}_{\mathrm{c2}}$ arise from the last two terms on the right-hand side of Eq. (25) and $\mathrm{d}\mathbf{u}_{\mathrm{c}}$ has the same form as in definition (15). On the other hand, if Eq. (10) and

$$\left({}^{t}\mathbf{x}^{\mathrm{t}} - {}^{t}\mathbf{x}^{\mathrm{h}}\right) \cdot \mathrm{d}^{t}\mathbf{n} = 0 \tag{27}$$

are considered, we have

$$\mathrm{d}^{t}g = {}^{t}\mathbf{n}^{\mathrm{T}}\, \mathbf{M}\, \mathrm{d}\mathbf{u}_{\mathrm{c}} \tag{28}$$

for the penetration. Finally, if the Lagrange multiplier method is used, combining Eqs. (26) and (28) gives

$$[\mathbf{k}_{\mathrm{c}}] \begin{Bmatrix} \mathrm{d}\mathbf{u}_{\mathrm{c}} \\ \mathrm{d}^{t}f_{\mathrm{n}}^{\mathrm{t}} \end{Bmatrix} = \begin{Bmatrix} \mathrm{d}^{t}\mathbf{f}_{\mathrm{c}} \\ \mathrm{d}^{t}g \end{Bmatrix} \tag{29}$$

$$[\mathbf{k}_{\mathrm{c}}] = \begin{bmatrix} \mathbf{k}_{\mathrm{c1}} + \mathbf{k}_{\mathrm{c2}} & \mathbf{M}^{\mathrm{T}}\, {}^{t}\mathbf{n} \\ {}^{t}\mathbf{n}^{\mathrm{T}}\, \mathbf{M} & \mathbf{0} \end{bmatrix} \tag{30}$$

for a particular node-segment pair.

For the whole contact system with elasto-plastic large deformation, the incremental strategy is usually used. For the i-th increment, the displacement increment $\Delta\mathbf{U}_i$ satisfying the incremental equilibrium equation

$$\Delta\mathbf{Q}_i - \Delta\mathbf{F}_{ci} = \Delta\mathbf{F}_i \tag{31}$$

is solved iteratively:

$$\left(\begin{bmatrix} \mathbf{K} & \mathbf{0} \\ \mathbf{0} & \mathbf{0} \end{bmatrix} - [\mathbf{K}_c] \right) \begin{Bmatrix} \Delta \mathbf{U}_i^{(j)} \\ \Delta \mathbf{F}_{ni}^{t(j)} \end{Bmatrix} = \begin{Bmatrix} \Delta \mathbf{F}_i \\ \mathbf{0} \end{Bmatrix} - \begin{Bmatrix} \Delta \mathbf{Q}_i^{(j-1)} \\ \mathbf{0} \end{Bmatrix} + \begin{Bmatrix} \Delta \mathbf{F}_{ci}^{(j-1)} \\ \Delta \mathbf{G}_i^{(j-1)} \end{Bmatrix}, \tag{32}$$

$$\Delta \mathbf{Q}_i^{(0)} = \mathbf{0}, \quad \Delta \mathbf{F}_{ci}^{(0)} = \mathbf{0}, \quad \Delta \mathbf{G}_i^{(0)} = \mathbf{0}, \tag{33}$$

$$\Delta \mathbf{U}_i = \sum_j \Delta \mathbf{U}_i^{(j)}, \quad \Delta \mathbf{F}_{ni}^{t} = \sum_j \Delta \mathbf{F}_{ni}^{t(j)}, \tag{34}$$

where the right superscript in parenthesis indicates the iteration in each increment, $\Delta \mathbf{Q}_i$ and $\Delta \mathbf{F}_i$ represent equivalent internal and applied nodal forces resulting from the discretization of virtual work, and $\Delta \mathbf{F}_{ni}^{t}$ and $\Delta \mathbf{F}_{ci}$ denote concentrated contact force on the target point and nodal contact force in incremental form. Tangent stiffness $\mathbf{K}$ is obtained from the derivative of internal force with respect to nodal displacement. $\mathbf{K}_c$ is given by the assemblage of $\mathbf{k}_c$ (Eq. (30)) for the whole contact system.

In the case of the penalty method, the contact constraint is approximately satisfied by introducing the penalty parameter α and defining the contact force at a target point as

$${}^{t}f_n^{t} = -\alpha {}^{t}g\,. \tag{35}$$

Using Eqs. (28) and (35), the first term on the right-hand side of Eq. (26) now becomes

$$\mathrm{d}{}^{t}f_n^{t}\, \mathbf{M}^{\mathrm{T}}\, {}^{t}\mathbf{n} = \mathbf{k}_{c3}\, \mathrm{d}\mathbf{u}_c\,, \tag{36}$$

where

$$\mathbf{k}_{c3} = -\alpha \mathbf{M}^{\mathrm{T}}\, {}^{t}\mathbf{n}\, {}^{t}\mathbf{n}^{\mathrm{T}}\, \mathbf{M}\,. \tag{37}$$

It is seen from Eqs. (18) and (35) that the contact force can be directly expressed as a function of the current nodal coordinate, i.e., a function of the displacement, and no extra variable is introduced. The linearized form of the equilibrium equation is given by

$$[\mathbf{k}_c]\, \mathrm{d}\mathbf{u}_c = \mathrm{d}{}^{t}\mathbf{f}_c\,, \tag{38}$$

$$[\mathbf{k}_c] = [\mathbf{k}_{c1} + \mathbf{k}_{c2} + \mathbf{k}_{c3}]\,. \tag{39}$$

Calculation of incremental displacement $\Delta \mathbf{U}_i$ for the whole contact system can now be carried out as follows.

$$([\mathbf{K}] - [\mathbf{K}_c]) \left\{ \Delta \mathbf{U}_i^{(j)} \right\} = \{\Delta \mathbf{F}_i\} - \left\{ \Delta \mathbf{Q}_i^{(j-1)} \right\} + \left\{ \Delta \mathbf{F}_{ci}^{(j-1)} \right\}, \tag{40}$$

$$\Delta \mathbf{Q}_i^{(0)} = \mathbf{0}, \quad \Delta \mathbf{F}_{ci}^{(0)} = \mathbf{0}, \tag{41}$$

$$\Delta \mathbf{U}_i = \sum_j \Delta \mathbf{U}_i^{(j)}\,. \tag{42}$$

Although a consistent contact stiffness theoretically ensures quadratic convergence in iterative solution procedure, such convergence may not always occur for a contact problem with large sliding, i.e., the contact boundaries in finite element analysis are divided into discrete segments, and during an iteration the normal vector can change discontinuously when a hitting node moves from one target segment to another. In this case, the iteration may not lead to a converged solution. In the present computation, the contact conditions of the hitting nodes are checked during an iteration, i.e., if tension occurs, then the contacting nodes are released. For elasto-plastic contact problems, such "jumps" in the contact conditions and/or normal vectors may cause unreasonable changes in the material properties at the integration points, which retard or prevent the convergence of the iterative calculation. Although in most cases these drawbacks can be overcome by choosing a small enough increment, the computational efficiency must then be considered since it can be substantially degraded as a result.

3. SENSITIVITY ANALYSIS FORMULATION

Deriving an expression for the response variation of a contact system with respect to design parameters is the main objective of this research, although attention will only be focused on frictionless contact problems.

For path-dependent problems, the incremental form of the equilibrium equation, which can be written at the i-th increment as

$$\Delta \mathbf{Q}_i - \Delta \mathbf{F}_{ci} = \Delta \mathbf{F}_i \,, \tag{43}$$

is usually used. Design parameters are denoted as b_j $(j = 1, ..., m)$. For simplicity of formulation, it is assumed that the external load is independent of the considered design parameters since the formulation based on this assumption can be easily extended to the general case. Taking the variation of Eq. (43) with respect to b_j gives

$$\frac{\mathrm{d}\Delta \mathbf{Q}_i}{\mathrm{d}b_j}\delta b_j - \frac{\mathrm{d}\Delta \mathbf{F}_{ci}}{\mathrm{d}b_j}\delta b_j = \left(\frac{\mathrm{d}\mathbf{Q}_i}{\mathrm{d}b_j} - \frac{\mathrm{d}\mathbf{F}_{ci}}{\mathrm{d}b_j}\right)\delta b_j - \left(\frac{\mathrm{d}\mathbf{Q}_{i-1}}{\mathrm{d}b_j} - \frac{\mathrm{d}\mathbf{F}_{ci-1}}{\mathrm{d}b_j}\right)\delta b_j = 0 \,. \tag{44}$$

Variations of internal and contact forces vanish at the beginning of the current increment where the equilibrium state was reached. Hence, Eq. (44) becomes

$$\left(\frac{\mathrm{d}\mathbf{Q}_i}{\mathrm{d}b_j} - \frac{\mathrm{d}\mathbf{F}_{ci}}{\mathrm{d}b_j}\right)\delta b_j = 0 \,. \tag{45}$$

Variations of the nodal internal forces with respect to design parameters can be evaluated as follows:

$$\frac{\mathrm{d}\mathbf{Q}_i}{\mathrm{d}b_j}\delta b_j = \mathbf{K}\,\delta \mathbf{U}_i + \underline{\delta}\mathbf{R}_i \,, \tag{46}$$

where

$$\mathbf{K} = \frac{\partial \mathbf{Q}_i}{\partial \mathbf{U}_i} \,, \tag{47}$$

$$\underline{\delta}\mathbf{R}_i = \frac{\partial \mathbf{Q}_i}{\partial \mathbf{U}_{i-1}}\delta \mathbf{U}_{i-1} + \frac{\partial \mathbf{Q}_i}{\partial b_j}\delta b_j \,. \tag{48}$$

Here $\mathbf{K}$ is the tangent stiffness and $\underline{\delta}\mathbf{R}_i$ is the variation of internal force in which the displacement is fixed to be that in the original system. In the present paper $\underline{\delta}\mathbf{R}_i$ is numerically evaluated using the procedure described in [2, 3]. The key problem considered here is how to treat variations of the nodal contact forces with respect to design parameters. Clearly, the treatment of such variations in contact problems depends on the contact constraint method adopted in the finite element analysis procedure. Therefore the following sensitivity analysis formulation will focus on how to treat contact forces and constraint conditions in the two constraint methods.

3.1. Sensitivity analysis using Lagrange multiplier method

In the Lagrange multiplier method, the additional independent variables, i.e., the Lagrange multipliers are introduced which are equivalent to the contact forces acting at a target point. The governing equation consists of Eq. (43) and the nonpenetration condition of a node-segment pair (a hitting node and target segment) at time step i, i.e.,

$$g_i\left(\mathbf{u}_{ci}(b_j), b_j\right) = 0 \,. \tag{49}$$

When considering a single node-segment pair, the equivalent nodal contact force $\mathbf{f}_{ci}$ is only a function of the nodal displacement $\mathbf{u}_{ci}$ and design parameters b_j, and thus

$$\mathbf{f}_{ci} = \mathbf{f}_{ci}\left(\mathbf{u}_{ci}(b_j), b_j\right) = \mathbf{M}^{\mathrm{T}}\,\mathbf{n}_i\, f_{ni}^{\mathrm{t}}\,, \tag{50}$$

$$f_{ni}^{\mathrm{t}} = f_{ni}^{\mathrm{t}}(b_j)\,, \tag{51}$$

where f_{ni}^{t} denotes the Lagrange multiplier at the i-th time step, which is only dependent on b_j, and $\mathbf{u}_{ci}$ is defined as in Eq. (15).

Let us first consider the contact force and contact constraint. By differentiating Eq. (50) and the nonpenetration condition

$$g_i\left(\mathbf{u}_{ci}(b_j), b_j\right) = \mathbf{n}_i^{\mathrm{T}}\,\mathbf{M}\,\mathbf{x}_{ci} = 0\,, \tag{52}$$

we obtain

$$\frac{\mathrm{d}\mathbf{f}_{ci}}{\mathrm{d}b_j} = \frac{\mathrm{d}f_{ni}^{\mathrm{t}}}{\mathrm{d}b_j}\,\mathbf{M}^{\mathrm{T}}\,\mathbf{n}_i + f_{ni}^{\mathrm{t}}\,\frac{\partial \mathbf{M}^{\mathrm{T}}}{\partial \mathbf{u}_{ci}}\,\mathbf{n}_i\,\frac{\mathrm{d}\mathbf{u}_{ci}}{\mathrm{d}b_j} + f_{ni}^{\mathrm{t}}\,\mathbf{M}^{\mathrm{T}}\,\frac{\partial \mathbf{n}_i}{\partial \mathbf{u}_{ci}}\,\frac{\mathrm{d}\mathbf{u}_{ci}}{\mathrm{d}b_j} + f_{ni}^{\mathrm{t}}\,\frac{\partial}{\partial b_j}\left(\mathbf{M}^{\mathrm{T}}\,\mathbf{n}_i\right) \tag{53}$$

and

$$\frac{\mathrm{d}g_i}{\mathrm{d}b_j} = \frac{\partial g_i}{\partial \mathbf{x}_{ci}}\,\frac{\mathrm{d}\mathbf{x}_{ci}}{\mathrm{d}b_j} + \frac{\partial g_i}{\partial b_j} = \mathbf{n}_i^{\mathrm{T}}\,\mathbf{M}\,\frac{\mathrm{d}\mathbf{u}_{ci}}{\mathrm{d}b_j} + \frac{\partial g_i}{\partial b_j} = 0\,. \tag{54}$$

Then, using the definitions

$$\mathbf{k}_{c1} = f_{ni}^{\mathrm{t}}\,\frac{\partial \mathbf{M}^{\mathrm{T}}}{\partial \mathbf{u}_{ci}}\mathbf{n}_i\,, \tag{55}$$

$$\mathbf{k}_{c2} = f_{ni}^{\mathrm{t}}\,\mathbf{M}^{\mathrm{T}}\,\frac{\partial \mathbf{n}_i}{\partial \mathbf{u}_{ci}}\,, \tag{56}$$

$$\frac{\partial \mathbf{f}_{di}}{\partial b_j} = f_{ni}^{\mathrm{t}}\,\frac{\partial}{\partial b_j}\left(\mathbf{M}^{\mathrm{T}}\,\mathbf{n}_i\right) \tag{57}$$

and combining them with Eqs. (53) and (54) gives

$$[\mathbf{k}_{\mathrm{c}}]\begin{Bmatrix} \dfrac{\mathrm{d}\mathbf{u}_{ci}}{\mathrm{d}b_j} \\ \dfrac{\mathrm{d}f_{ni}^{\mathrm{t}}}{\mathrm{d}b_j} \end{Bmatrix} = \begin{Bmatrix} \dfrac{\mathrm{d}\mathbf{f}_{ci}}{\mathrm{d}b_j} - \dfrac{\partial \mathbf{f}_{di}}{\partial b_j} \\ -\dfrac{\partial g_i}{\partial b_j} \end{Bmatrix}, \tag{58}$$

where

$$[\mathbf{k}_{\mathrm{c}}] = \begin{bmatrix} \mathbf{k}_{c1} + \mathbf{k}_{c2} & \mathbf{M}^{\mathrm{T}}\,\mathbf{n}_i \\ \mathbf{n}_i^{\mathrm{T}}\,\mathbf{M} & \mathbf{0} \end{bmatrix}. \tag{59}$$

By comparing the first three terms on the right-hand side of Eq. (53) with the right-hand side of Eq. (25), and Eq. (59) with Eq. (30), it is found that matrix $\mathbf{k}_{\mathrm{c}}$ is the same as the consistent contact tangent stiffness in the finite element analysis. This indicates that, in a contact problem, $\mathbf{k}_{\mathrm{c}}$ must be used in both the finite element analysis and the sensitivity analysis.

Equations (53)–(59) can only be applied to a single node-segment pair. Thus, assembling Eq. (58) for an entire contact system yields

$$\begin{Bmatrix} \dfrac{\mathrm{d}\mathbf{F}_{ci}}{\mathrm{d}b_j} \\ \mathbf{0} \end{Bmatrix} - [\mathbf{K}_{\mathrm{c}}]\begin{Bmatrix} \dfrac{\mathrm{d}\mathbf{U}_i}{\mathrm{d}b_j} \\ \dfrac{\mathrm{d}\mathbf{F}_{ni}^{\mathrm{t}}}{\mathrm{d}b_j} \end{Bmatrix} = \begin{Bmatrix} \dfrac{\partial \mathbf{F}_{di}}{\partial b_j} \\ \dfrac{\partial \mathbf{G}_i}{\partial b_j} \end{Bmatrix}. \tag{60}$$

Substituting Eqs. (46) and (60) into Eq. (45) leads

$$\left(\begin{bmatrix} \mathbf{K} & \mathbf{0} \\ \mathbf{0} & \mathbf{0} \end{bmatrix} - [\mathbf{K}_{\mathrm{c}}] \right) \begin{Bmatrix} \delta \mathbf{U}_i \\ \delta \mathbf{F}^{\mathrm{t}}_{\mathrm{n}i} \end{Bmatrix} = \begin{Bmatrix} \underline{\delta} \mathbf{F}_{\mathrm{d}i} - \underline{\delta} \mathbf{R}_i \\ \underline{\delta} \mathbf{G}_i \end{Bmatrix}, \tag{61}$$

where the operator $\underline{\delta}$ denotes $\partial / \partial b_j \cdot \delta b_j$. If the terms $\underline{\delta} \mathbf{F}_{\mathrm{d}i}$ and $\underline{\delta} \mathbf{G}_i$ are evaluated, the sensitivities of the displacement and the Lagrange multiplier can be determined without using an iterative operation by utilizing the inverse of the stiffness matrix obtained at the end of current increment in the finite element analysis. The sensitivities of strain, stress, and reaction force can then be sequentially computed. The evaluation of $\underline{\delta} \mathbf{F}_{\mathrm{d}i}$ and $\underline{\delta} \mathbf{G}_i$ will be discussed in the next section.

As a special case, let us consider a non-shape sensitivity analysis problem where the initial shape of structure is not related to any design variable. In this case, we have

$$\mathbf{x}_{\mathrm{c}i} = \mathbf{x}_{\mathrm{c}0} + \mathbf{u}_{\mathrm{c}i}\,, \tag{62}$$

$$\frac{\partial \mathbf{x}_{\mathrm{c}i}}{\partial b_j} = \frac{\partial \mathbf{x}_{\mathrm{c}0}}{\partial b_j} = \mathbf{0}\,, \tag{63}$$

$$\frac{\partial}{\partial b_j} \left(\mathbf{M}^{\mathrm{T}} \mathbf{n}_i \right) = \mathbf{0}\,, \tag{64}$$

where $\mathbf{x}_{\mathrm{c}0}$ and $\mathbf{x}_{\mathrm{c}i}$ respectively denote the initial coordinates of the contact node and those at time step i. Therefore

$$\frac{\partial g_i}{\partial b_j} = \mathbf{n}_i{}^{\mathrm{T}} \mathbf{M} \frac{\mathrm{d}\mathbf{x}_{\mathrm{c}i}}{\mathrm{d}b_j} = 0\,, \tag{65}$$

$$\frac{\partial \mathbf{f}_{\mathrm{d}i}}{\partial b_j} = \mathbf{0} \tag{66}$$

hold and Eq. (61) can be simplified as

$$\left(\begin{bmatrix} \mathbf{K} & \mathbf{0} \\ \mathbf{0} & \mathbf{0} \end{bmatrix} - [\mathbf{K}_{\mathrm{c}}] \right) \begin{Bmatrix} \delta \mathbf{U}_i \\ \delta \mathbf{F}^{\mathrm{t}}_{\mathrm{n}i} \end{Bmatrix} = \begin{Bmatrix} -\underline{\delta} \mathbf{R}_i \\ \mathbf{0} \end{Bmatrix}, \tag{67}$$

where only $\underline{\delta} \mathbf{R}_i$ needs to be determined.

3.2. Sensitivity analysis using penalty method

In the penalty method, a contact problem is transformed into an unconstrained problem by introducing a penalty factor α. The contact force at a target point is not an independent variable, but a function of displacement that can be expressed at increment i as

$$f^{\mathrm{t}}_{\mathrm{n}i} \left(\mathbf{u}_{\mathrm{c}i}(b_j), b_j \right) = -\alpha g_i \left(\mathbf{u}_{\mathrm{c}i}(b_j), b_j \right) = -\alpha \mathbf{n}_i{}^{\mathrm{T}}\, \mathbf{M}\, \mathbf{x}_{\mathrm{c}i}\,, \tag{68}$$

where $\mathbf{M}$ and $\mathbf{x}_{\mathrm{c}i}$ are defined as in Eqs. (14) and (19).

Referring to Eq. (68), Eq. (53) becomes

$$\begin{aligned} \frac{\mathrm{d}\mathbf{f}_{\mathrm{c}i}}{\mathrm{d}b_j} = {} & -\alpha \mathbf{M}^{\mathrm{T}}\, \mathbf{n}_i\, \mathbf{n}_i{}^{\mathrm{T}}\, \mathbf{M} \frac{\mathrm{d}\mathbf{u}_{\mathrm{c}i}}{\mathrm{d}b_j} + f^{\mathrm{t}}_{\mathrm{n}i} \frac{\partial \mathbf{M}^{\mathrm{T}}}{\partial \mathbf{u}_{\mathrm{c}i}} \mathbf{n}_i \frac{\mathrm{d}\mathbf{u}_{\mathrm{c}i}}{\mathrm{d}b_j} + f^{\mathrm{t}}_{\mathrm{n}i} \mathbf{M}^{\mathrm{T}} \frac{\partial \mathbf{n}_i}{\partial \mathbf{u}_{\mathrm{c}i}} \frac{\mathrm{d}\mathbf{u}_{\mathrm{c}i}}{\mathrm{d}b_j} \\ & -\alpha \frac{\partial g_i}{\partial b_j} \mathbf{M}^{\mathrm{T}} \mathbf{n}_i - \alpha g_i \frac{\partial}{\partial b_j} \left(\mathbf{M}^{\mathrm{T}} \mathbf{n}_i \right) \end{aligned} \tag{69}$$

and using the following definitions

$$\mathbf{k}_c = -\alpha \mathbf{M}^T \mathbf{n}_i \mathbf{n}_i^T \mathbf{M} + f_{ni}^t \frac{\partial \mathbf{M}^T}{\partial \mathbf{u}_{ci}} \mathbf{n}_i + f_{ni}^t \mathbf{M}^T \frac{\partial \mathbf{n}_i}{\partial \mathbf{u}_{ci}}$$

$$= \mathbf{k}_{c1} + \mathbf{k}_{c2} + \mathbf{k}_{c3}\,, \tag{70}$$

$$\frac{\partial \mathbf{f}_{pi}}{\partial b_j} = -\alpha \frac{\partial g_i}{\partial b_j} \mathbf{M}^T \mathbf{n}_i\,, \tag{71}$$

$$\frac{\partial \mathbf{f}_{di}}{\partial b_j} = -\alpha g_i \frac{\partial}{\partial b_j} \left(\mathbf{M}^T \mathbf{n}_i \right)\,, \tag{72}$$

we obtain

$$\frac{\mathrm{d}\mathbf{f}_{ci}}{\mathrm{d}b_j} = \mathbf{k}_c \frac{\mathrm{d}\mathbf{u}_{ci}}{\mathrm{d}b_j} + \frac{\partial \mathbf{f}_{pi}}{\partial b_j} + \frac{\partial \mathbf{f}_{di}}{\partial b_j}\,. \tag{73}$$

Once again note that $\mathbf{k}_c$ is the same as the matrix defined by Eq. (39); thereby indicating that consistent contact stiffness must also be used in the sensitivity analysis just as in the finite element analysis.

Since Eqs. (69)–(73) only apply to a single node-segment pair, they need to be assembled to treat the whole contact system, i.e.,

$$\frac{\mathrm{d}\mathbf{F}_{ci}}{\mathrm{d}b_j} = \mathbf{K}_c \frac{\mathrm{d}\mathbf{U}_i}{\mathrm{d}b_j} + \frac{\partial \mathbf{F}_{pi}}{\partial b_j} + \frac{\partial \mathbf{F}_{di}}{\partial b_j}\,. \tag{74}$$

As in the case of using the Lagrange multiplier method, substituting Eq. (74) into Eq. (45) and writing the result in the variational form, we have

$$(\mathbf{K} - \mathbf{K}_c)\, \delta \mathbf{U}_i = -\underline{\delta} \mathbf{R}_i + \underline{\underline{\delta}} \mathbf{F}_{pi} + \underline{\underline{\delta}} \mathbf{F}_{di}\,. \tag{75}$$

If $\underline{\underline{\delta}} \mathbf{F}_{pi}$ and $\underline{\underline{\delta}} \mathbf{F}_{di}$ are calculated, the sensitivity of displacement can be given as

$$\delta \mathbf{U}_i = (\mathbf{K} - \mathbf{K}_c)^{-1} \left(-\underline{\delta} \mathbf{R}_i + \underline{\underline{\delta}} \mathbf{F}_{pi} + \underline{\underline{\delta}} \mathbf{F}_{di} \right) \tag{76}$$

and consequently the sensitivities of strain, stress and reaction force can be determined. It is clear that iterative operation is unnecessary in the above because $(\mathbf{K} - \mathbf{K}_c)^{-1}$ was obtained in the finite element analysis.

In the special case of non-shape sensitivity analysis problems, the partial derivative of the penetration vanishes, and thus

$$\frac{\partial \mathbf{F}_{pi}}{\partial b_j} = \mathbf{0}\,, \tag{77}$$

$$\frac{\partial \mathbf{F}_{di}}{\partial b_j} = \mathbf{0}\,. \tag{78}$$

Hence Eq. (75) is simplified to

$$(\mathbf{K} - \mathbf{K}_c)\, \delta \mathbf{U}_i = -\underline{\delta} \mathbf{R}_i\,. \tag{79}$$

It should be noted that $\underline{\underline{\delta}} \mathbf{F}_{di}$ has the same form in both formulations of the constraint method. In addition, although $\underline{\delta} \mathbf{G}_i$ and $\underline{\underline{\delta}} \mathbf{F}_{pi}$ appear to be different in each formulation, at an element level they actually have the same meaning, i.e., the variation of penetration g_i.

3.3. Conditional variations of contact force/constraint

The basic equations related to the two contact constraint methods considered (Eqs. (61) and (75)) have been derived for use in the sensitivity analysis algorithm. Their stiffness matrices on the left-hand side have the same form as those obtained by the finite element analysis at the end of the current increment, i.e., the tangent stiffness at the convergence of iteration. This implies that after the analysis of the original system, the sensitivity analysis can be carried out by solving a system of linear equations without iteration, providing the terms on the right-hand side of these equations can be evaluated. The contact state in the sensitivity analysis stage is identified in accordance with the state determined by the finite element analysis of the original system. In the formulations of the contact constraint methods, it can be seen that the right-hand sides of Eqs. (61) and (75) are partial variations in which the displacement is fixed to be that of the original system; hence they are also termed conditional variations. In the present paper, the conditional variation of the internal force $\underline{\delta}\mathbf{R}_i$ is numerically evaluated as shown in [2, 3].

Before calculating $\underline{\delta}\mathbf{f}_{di}$ and $\underline{\delta}\mathbf{g}_i$, their physical implication will be studied. It is clear from Eq. (50) that the contact nodal force ${}^t\mathbf{f}_c$ is dependent on the location of the target point, which determines the normal vector ${}^t\mathbf{n}$ and the local coordinates included in $\mathbf{M}$. Due to variations in the initial shape, the location of the target point in a perturbed system is changed even if the displacement and contact force at the target point remain the same as in the original system. Hence the contact nodal force is also changed, where $\underline{\delta}\mathbf{f}_{di}$, defined as $f_{ni}^t\underline{\delta}(\mathbf{M}^T\mathbf{n}_i)$, indicates this change. On the other hand, a variation in the initial shape leads to the nonpenetration condition not being satisfied when using the displacement of the original system, where $\underline{\delta}\mathbf{g}_i$ indicates this behavior. The conditional variations represented by these two terms result in an unbalanced contact force in the perturbed system that must be compensated for.

Figure 2 schematically shows the mechanism of sensitivity analysis in a contact problem using the Lagrange multiplier contact constraint. The indicated reaction force is considered as a response surface, being a function of the displacement and the Lagrange multiplier, i.e., the contact force at the target point. The response surfaces of the original and perturbed systems are respectively denoted by S_o and S_p. It should be noted that the solution of the problem is not unique if only the

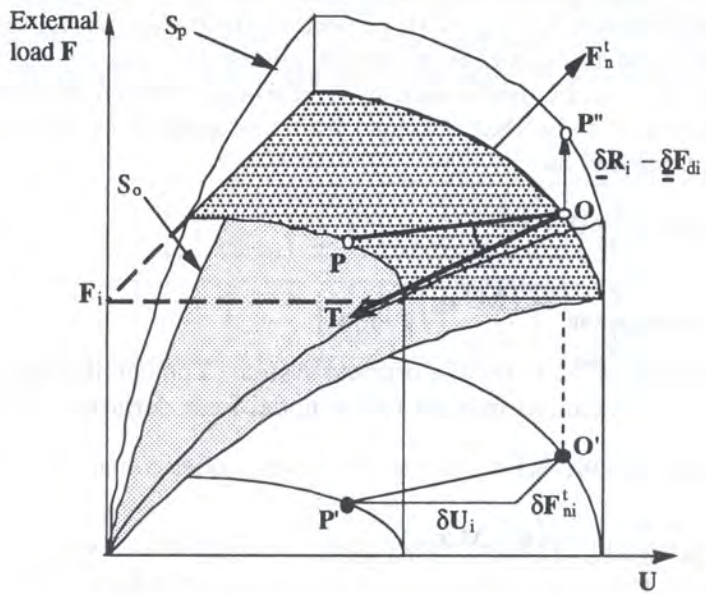

Fig. 2. Mechanism of sensitivity analysis for contact problem using Lagrange multiplier constraint

external load $\mathbf{F}$ is given, and that the kinematic contact condition must be satisfied to determine it. The solution points for the original and perturbed systems are indicated as points **O** and **P**. Their

projections on the $\mathbf{U} - \mathbf{F}_{\mathrm{n}}^{\mathrm{t}}$ plane are $\mathbf{O}'$ and $\mathbf{P}'$, where $\mathbf{F}_{\mathrm{n}}^{\mathrm{t}}$ is the assembled Lagrange multiplier vector for the whole system. Fixing the displacement and the Lagrange multiplier with those of the original system gives the state point of the perturbed system $\mathbf{P}''$, which will lead to obtaining the unbalanced force $\underline{\delta}\mathbf{F}_{\mathrm{d}i} - \underline{\delta}\mathbf{R}_i$. To compensate this unbalanced force, the state point must be transformed back to point $\mathbf{P}$. On any smooth surface, there exists a tangential plane at point $\mathbf{O}$, and in fact, this plane is determined by the tangent stiffness $\mathbf{K}$ and the assemblage of $\mathbf{k}_{\mathrm{c}1}$, $\mathbf{k}_{\mathrm{c}2}$ defined in Eqs. (55), (56). The direction of transformation back to the state point $\mathbf{P}$ may be indicated by the tangential plane, but it is not unique. However, it can be uniquely determined using the nonpenetration condition which requires the state point to be returned in the direction of $\mathbf{T}$. Thus, the total variation $\mathbf{O} - \mathbf{P}$, i.e., the variations of displacement and the Lagrange multiplier, can be obtained from the conditional unbalanced force, $-(\underline{\delta}\mathbf{R}_i - \underline{\underline{\delta}}\mathbf{F}_{\mathrm{d}i})$, and the direction of $\mathbf{T}$. Determining the state point of the perturbed system in accordance with the direction $\mathbf{T}$ is equivalent to solving the equation system (61).

When using the penalty method for contact constraint, the reaction force is reduced to a function that is only dependent on displacement. Consequently, the unbalance due to the conditional variation of penetration is transformed into an additional conditional unbalanced force $\underline{\delta}\mathbf{f}_{\mathrm{p}i}$, defined as $-\alpha\mathbf{M}^{\mathrm{T}}\mathbf{n}_i\underline{\delta}\mathbf{g}_i$, and in this case, only the sensitivity of displacement needs to be computed.

Similarly to the sensitivity analysis for elasto-plastic problems, the conditional contact force variation can be treated by the analytical direct differentiation method. However, in contact problems the position of the target point and its normal vector change due to the variations of the design parameter. In addition, the changes are dependent on the variation of the internal force. Thus, when contact problems have complex contact boundaries, it is not easy to carry out this approach analytically.

Instead of using pure analytical method, a semi-analytical approach is adopted here which is consistent with that for elasto-plastic problems [2, 3]. In this approach, only the conditional variation of contact force is evaluated numerically by taking the difference between the perturbed and original systems, and the other formulation is analytically carried out. Hence the advantage of the direct differentiation method is preserved.

In finite element analysis of contact problems using the Lagrange multiplier constraint method, the contact forces at the target points are independent variables. The conditional variations of the equivalent nodal forces, denoted by $\underline{\delta}\mathbf{f}_{\mathrm{d}i}$, with respect to the design parameters are dependent on the conditional variations of the positions of target points, i.e., the conditional variation of the resultant deformation. $\underline{\delta}\mathbf{f}_{\mathrm{d}i}$ can be determined by perturbing a design parameter of the structure while fixing the displacement to be that obtained from the analysis of the original structure. The resultant difference is expressed as

$$\begin{aligned}\underline{\delta}\mathbf{f}_{\mathrm{d}i} &= \mathbf{f}_{\mathrm{d}i}\left(\mathbf{u}_{ci}^{\mathrm{o}}, b_j + \delta b_j\right) - \mathbf{f}_{\mathrm{d}i}\left(\mathbf{u}_{ci}^{\mathrm{o}}, b_j\right) \\ &= f_{\mathrm{n}i}^{\mathrm{t,o}}\left[\left(\mathbf{M}^{\mathrm{T}}\mathbf{n}_i\right)_{\mathbf{u}=\mathbf{u}_{ci}^{\mathrm{o}}, b_j+\delta b_j} - \left(\mathbf{M}^{\mathrm{T}}\mathbf{n}_i\right)_{\mathbf{u}=\mathbf{u}_{ci}^{\mathrm{o}}, b_j}\right],\end{aligned} \tag{80}$$

where the right superscript "o" denotes the original system. The conditional variation of the penetration can be obtained in a similar manner to the nodal force variation, i.e.,

$$\begin{aligned}\underline{\delta}\mathbf{g}_i &= g_i\left(\mathbf{u}_{ci}^{\mathrm{o}}, b_j + \delta b_j\right) - g_i\left(\mathbf{u}_{ci}^{\mathrm{o}}, b_j\right) \\ &= \left(\mathbf{n}_i^{\mathrm{T}}\mathbf{M}\mathbf{x}_{ci}\right)_{\mathbf{u}=\mathbf{u}_{ci}^{\mathrm{o}}, b_j+\delta b_j} - \left(\mathbf{n}_i^{\mathrm{T}}\mathbf{M}\mathbf{x}_{ci}\right)_{\mathbf{u}=\mathbf{u}_{ci}^{\mathrm{o}}, b_j}.\end{aligned} \tag{81}$$

For contact problem analysis using the penalty contact constraint, the contact force at the target point is transformed into a function of nodal displacement. The conditional variation of nodal contact force is subsequently obtained as

$$\underline{\delta}\mathbf{f}_{\mathrm{p}i} = -\alpha\left(\mathbf{M}^{\mathrm{T}}\mathbf{n}_i\right)_{\mathbf{u}=\mathbf{u}_{ci}^{\mathrm{o}}, b_j}\left[g_i\left(\mathbf{u}_{ci}^{\mathrm{o}}, b_j + \delta b_j\right) - g_i\left(\mathbf{u}_{ci}^{\mathrm{o}}, b_j\right)\right] \tag{82}$$

and

$$\underline{\delta}\mathbf{f}_{\mathrm{d}i} = -\alpha g_i^{\mathrm{o}} \left[\left(\mathbf{M}^{\mathrm{T}} \mathbf{n}_i \right)_{\mathbf{u}=\mathbf{u}_{ci}^{\mathrm{o}}, b_j + \delta b_j} - \left(\mathbf{M}^{\mathrm{T}} \mathbf{n}_i \right)_{\mathbf{u}=\mathbf{u}_{ci}^{\mathrm{o}}, b_j} \right] . \tag{83}$$

To calculate the conditional variations, the terms for the perturbed system are computed using the perturbed design parameters and the original system displacement. When treating the terms for the original system, it is important to consider the balance between computational efficiency and computer memory capacity, i.e., some terms required in the sensitivity analysis, such as $(\mathbf{M}^{\mathrm{T}}\mathbf{n}_i)_{\mathbf{u}=\mathbf{u}_{ci}^{\mathrm{o}}, b_j}$, may be stored in the finite element analysis stage, or they may be computed again in the sensitivity analysis stage. If a large-scale problem with a relatively small contact boundary is analyzed, then the latter is considered more efficient.

4. Numerical examples

In this section, a couple of numerical examples are presented. Firstly, a contact system comprised of two cantilever beams subjected to elasto-plastic large deformation is analyzed. The results obtained by an approximated contact stiffness, which is resulted from the assumption that during an iteration the location of target point and the normal vector remain constant, are compared with those by the consistent stiffness. The necessity of employing consistent contact tangent stiffness for reaching quadratic convergence, as well as its effect on the sensitivity analysis are examined. The second example applies the sensitivity analysis to a real problem of heat exchange tube and plate system. Close examination of the results provides practical design information. In these examples eight-node hexahedral elements are used for the spatial discretization and four-node segments for modeling the contact surface.

4.1. Two-cantilever-beam contact problem

This example analyses a two-cantilever-beam contact system with finite sliding and elasto-plasticity. Figure 3 shows the geometry of the model and its finite element meshes. The space of two beams is $t = 10$ mm. The Lagrange multiplier contact constraint method is applied. The displacements in

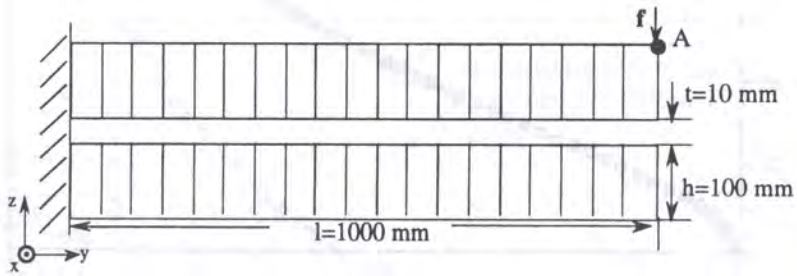

Fig. 3. Finite element model of two-cantilever-beam contact system

the x-direction are constrained to simulate a plane strain state. The material constants are given as $E = 200$ GPa, $\nu = 0.3$, hardening coefficient $H' = 2$ GPa, and yield stress $\sigma_{\mathrm{y}} = 0.2$ GPa. A concentrated external load $\mathbf{f}$ is applied at the point A. In this analysis, if the load increment is taken too large, the computation becomes unstable and divergent because the trial-and-error procedure used during an iteration causes an intense change of the state in the system. Thus, a relatively small concentrated load is applied ($f = 80$ kN) and is divided into 50 steps. Figure 4 shows the resultant deformation, where finite sliding is observed.

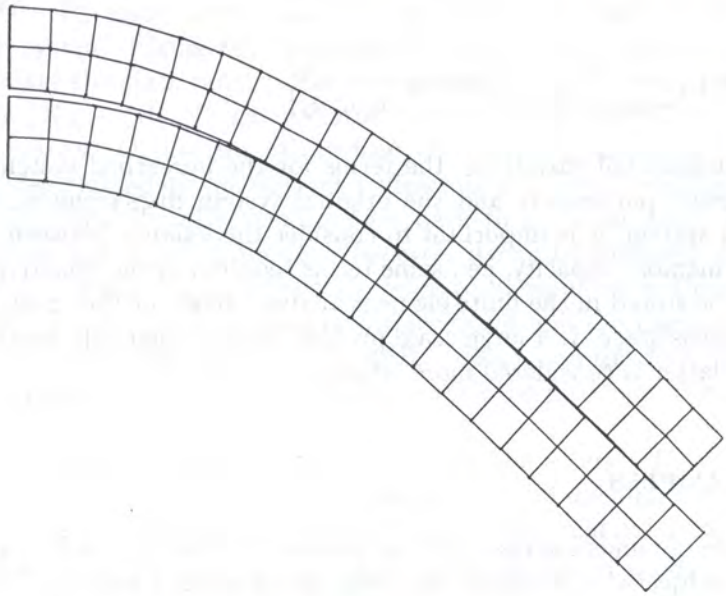

Fig. 4. Deformation of two beams

Figure 5 shows the load-displacement result, in which the contact system goes through a stiffen-soften-stiffen path. The yield points first appear in the upper beam, while the lower beam remains almost in elastic state. As the deformation increases, some points on the lower beam also yield, causing a softening of the contact system. Since the increase in the number of yield points is gradually reduced as the resisting moment simultaneously increases due to the sliding of the contact nodes, the contact system then stiffens again.

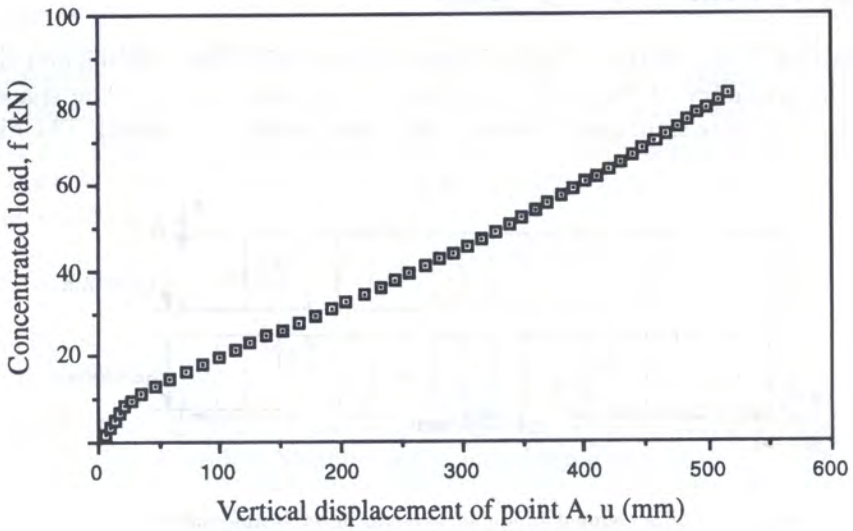

Fig. 5. Load–displacement curve of point A

The finite element analysis results obtained by the consistent stiffness were the same as those obtained by the approximated one since the given tolerance in a step was small enough. However, the solution obtained by the approximated contact stiffness takes 29 min CPU time to converge, while that by the consistent one takes about 19 min. Table 1 summarizes the convergence in the two cases for a typical step.

Table 1. Convergence of two-elasto-plastic-beam contact system in a typical step

Normalized energy residuals with the consistent contact stiffness:									
1.0e0	0.181	0.369e-4	0.319e-9	0.226e-18					
Normalized energy residuals with the approximated contact stiffness:									
1.0e0	0.239	0.430e-3	0.241e-5	0.399e-7	0.687e-9	0.118e-10	0.204e-12	0.351e-14	0.606e-16

The sensitivity of vertical displacement at point A is analyzed with respect to b, the normalized height of beams, i.e., $h = h_0(1 + b)$, and the results using both stiffness are shown in Figs. 6 and 7 together with those obtained by finite difference method (FDM). Since the results of finite element

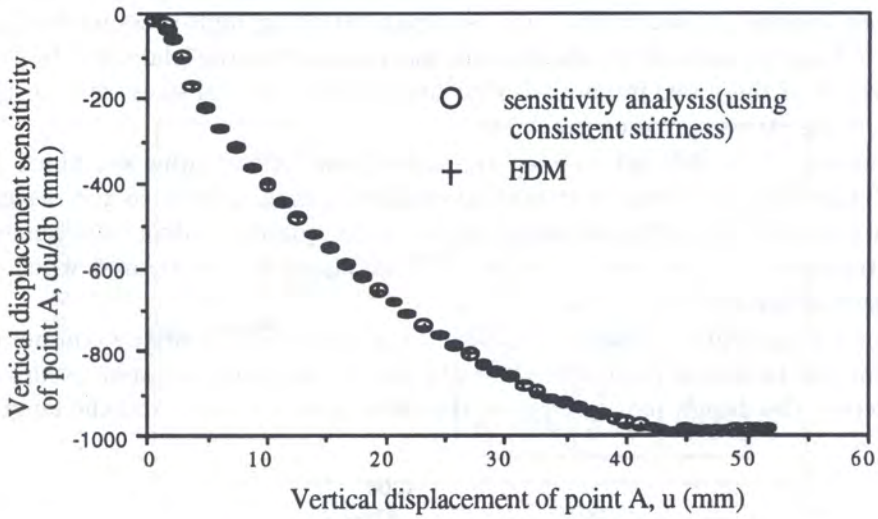

Fig. 6. Displacement sensitivity histories obtained by FDM and sensitivity analysis with consistent contact stiffness

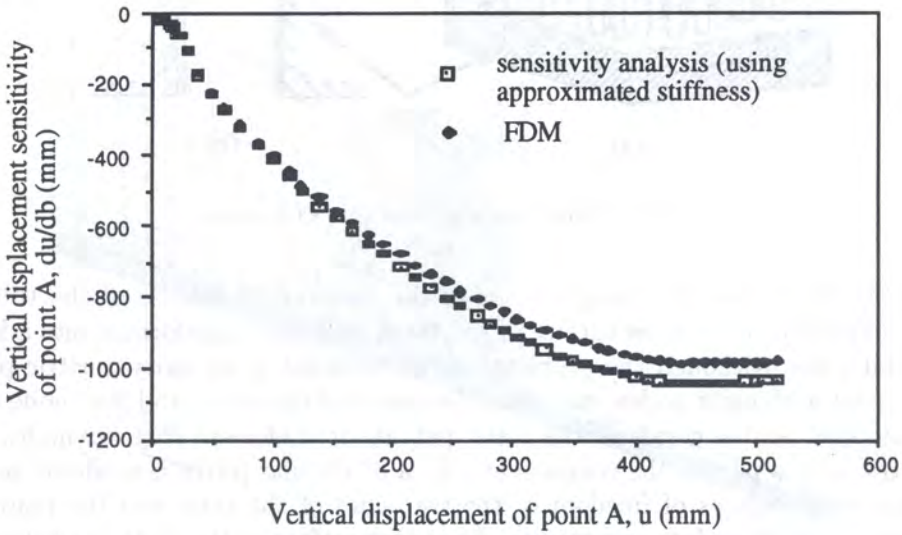

Fig. 7. Displacement sensitivity histories obtained by FDM and sensitivity analysis with approximated contact stiffness

analysis are not affected by the contact stiffness if the tolerance in a step is given small enough, then as expected, FDM yields the same sensitivities for both contact stiffness. In contrast, however, the results obtained by the sensitivity analysis method are affected by the contact stiffness used. Note that the consistent contact stiffness gives sensitivity results which agree well with those obtained by FDM, while errors arise in those with approximated stiffness. The negative sensitivities indicate that the increase in h will reduce the displacement, thereby stiffening the contact system.

4.2. Contact problem of heat exchange tube and plate

In chemical and nuclear power plants numerous shell-and-tube heat exchangers are used. The heat exchange tubes are joined to a thick plate by an expansion process, in which the conventional mechanical expansion method is most widely used. This joint is important because it forms a water- and air-tight seal at the interface between the tube and plate. Recently, the hydraulic expansion method has been applied, in which the tube is expanded using high-pressure liquid, after which the pressure is reduced to zero. The tube then forms a joint with the plate due to the spring-back force. The drawback of these two methods is that high tensile residual stress may result at the tube surface, which causes stress corrosion cracking.

During fabrication, it is difficult to keep the dimensions of the tube and thick plate at their design values. Thus, the variations of structural responses with respect to the design parameters must be known to ensure the safety of the plant and meet quality control requirements. Here, the effect of the dimensions of components on the residual stress is investigated when the hydraulic expansion method is applied.

Figure 8 shows a tube-plate system, and Fig. 9 the cross-section of the computational model used to represent the tube and plate. On the right side of the plate, a taper occurs as a result of the drilling process. The design parameters are the tube outer radius t_1 and the length and height

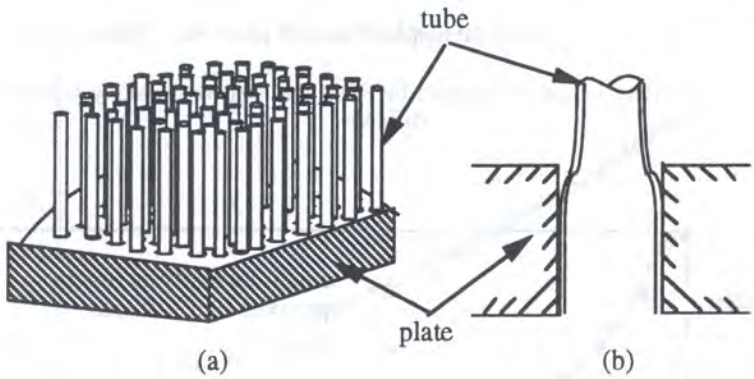

Fig. 8. Tube-plate system of heat exchanger

of the taper (Fig. 9), t_2 and t_3. Figure 10 shows the material properties of the tube and plate. The pressure is applied to the inner surface of the tube, and then transformed into a kinematically equivalent nodal force. Although the problem can be modeled as an axisymmetric problem, here hexahedral element with eight nodes, except at the corner of the plate, and four-node quadrilateral segment are adopted. At the corner of the plate, pentahedron element with six nodes is used. Due to the symmetry, only a part of the component, i.e., a 5° circular pitch, is modeled and computed. The nodal tangential degrees of freedom of the two sides of the tube and the plate are treated by applying symmetric boundary constraints. The outer surface of the plate is rigidly constrained. The left side of the contact system is constrained in the axial direction. Figure 11 shows the grid model.

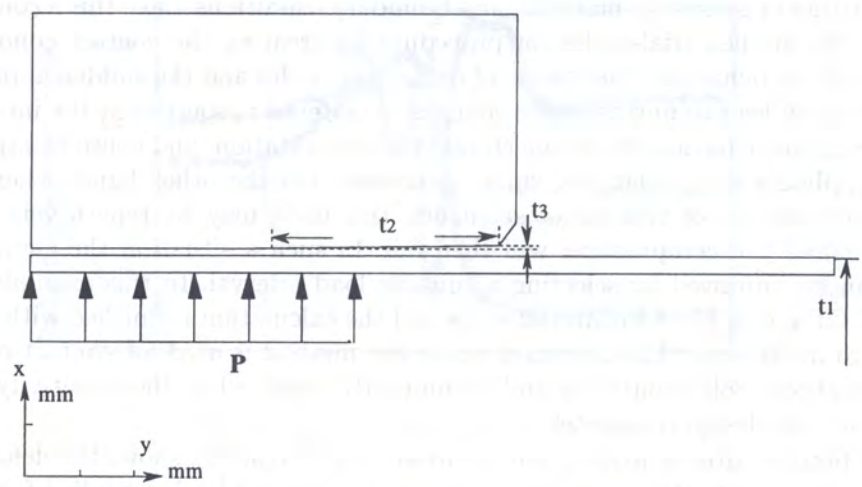

Fig. 9. Computational model of tube and plate

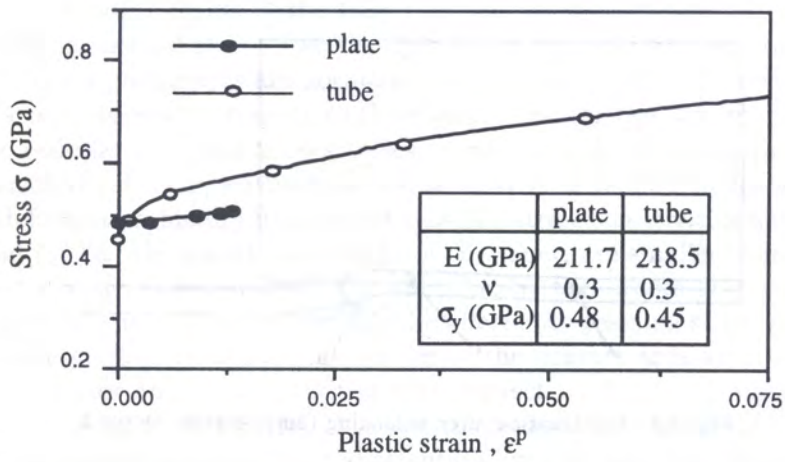

Fig. 10. Material properties of heat exchange tube-plate system

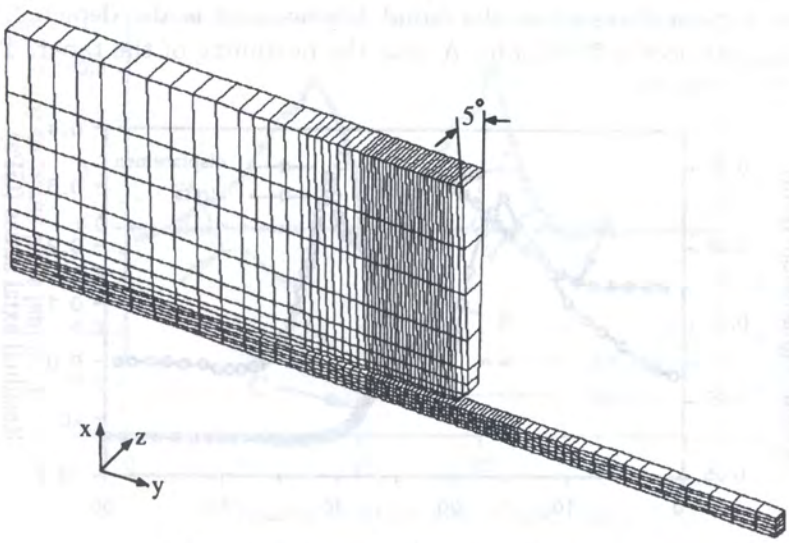

Fig. 11. Grid model of heat exchange tube-plate system

The nonlinearities of geometry, material, and boundary conditions make this a complex problem, especially since the applied trial-and-error procedure for treating the contact condition interacts with the elasto-plastic behavior. The release of contacting nodes and the sudden appearance of new contacting nodes may lead to unreasonable changes of material properties at the integration points near these nodes. This behavior affects the stability of computation, and consequently, the external load must be applied with a relatively small increment. On the other hand, when a contacting node is near the interface of two target segments, this node may be repetitively matched with another segment and the computation will then fail. In such a situation the convergence of the computation can be improved by selecting a suitable load interval. In this example, the external load, $P = 0.167$ GPa, is applied within 100 steps and the calculation is finished with the load being decreased to zero in 20 steps. The Lagrange multiplier method is used for contact constraint. The finite element analysis took about 6 hr and 20 min CPU time, while the sensitivity analysis took about 15 min for each design parameter.

The results obtained after unloading are discussed next. Figure 12 shows the deformation of the tube and plate (the amplification factor is 5), where the external load is applied from the left side up to point B. Point A represents the beginning of the taper, while point C gives the border of the contact area after unloading. Note that only a part of the plate is in contact with the tube.

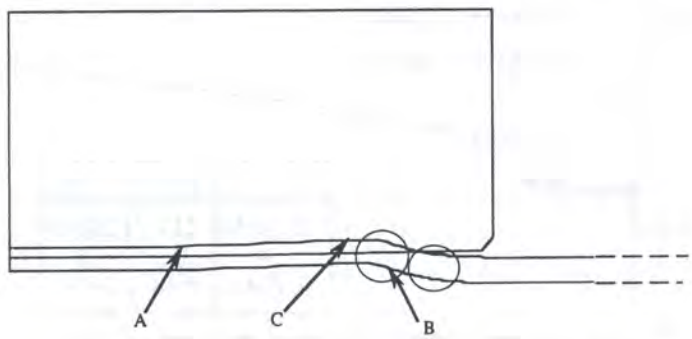

Fig. 12. Deformation after unloading (amplification factor 5)

The tube wall is clearly bent at two places due to the vanishing external load and the existence of a free boundary. Figures 13 and 14 respectively show the distributions of axial and hoop residual stresses on the inner tube surface, where the radial displacement is also depicted. As expected, the increase in displacement occurs from point A near the beginning of the taper. The displacements

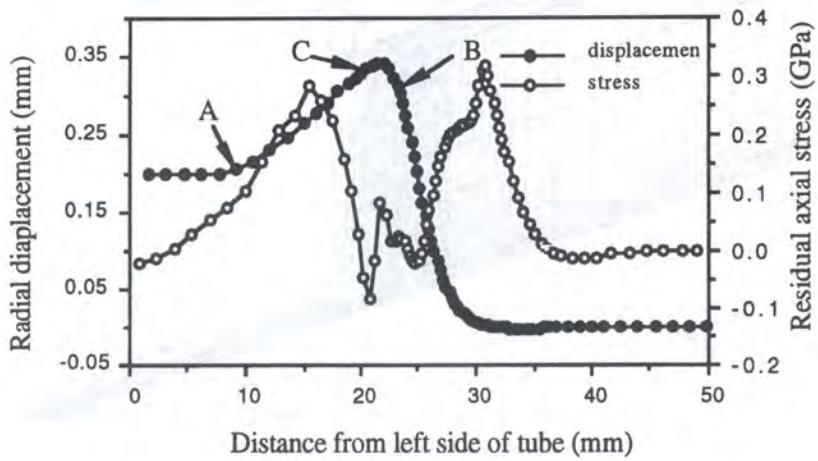

Fig. 13. Residual axial stress distribution on inner surface of tube

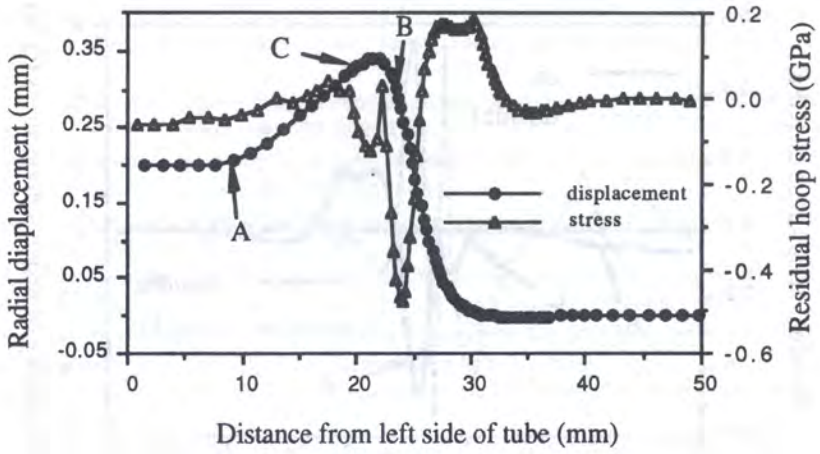

Fig. 14. Residual hoop stress distribution on inner surface of tube

near the right-hand side of the tube are almost zero. The residual axial and hoop stresses reach high values near the bending region of the tube.

The sensitivities of residual stresses are analyzed based on the formulation introduced in the previous section. Design parameters are normalized as $t_i = t_{i0}(1 + b_i)$. The results of residual axial and hoop stress sensitivities with respect to three design parameters are given in Figs. 15 and 16 together with the residual axial and hoop stresses, respectively. In this example the distribution of residual stress sensitivity is complex because the sensitivity is related to the state of the contact surface and the deformation history. It is noted that the stress sensitivities with respect to design parameters b_2 and b_3, i.e., the length and height of the taper, are smaller than those with respect to design parameter b_1, the outer diameter of the tube, by two orders of magnitude. This means that the variation of the outer diameter of the tube affects the residual stress remarkably. Another fact observed from Fig. 15 is that near the border of the contact area after unloading (point C) the residual axial stresses and its sensitivities with respect to design parameter b_1 both reach a relatively high value. Also from Fig. 16, this fact is observed near the end of the external load region (point B) for hoop component. Special attention must be paid to these points in design and quality control.

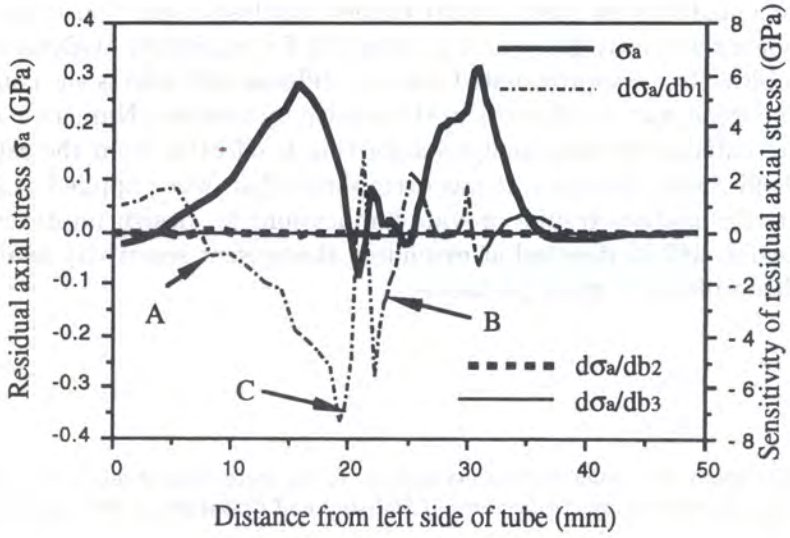

Fig. 15. Distribution of residual axial stress and sensitivity on inner surface of tube

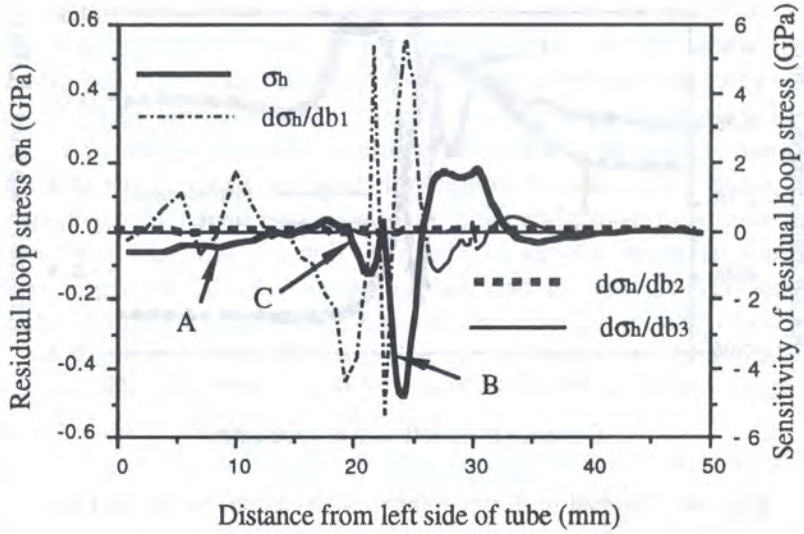

Fig. 16. Distribution of residual hoop stress and sensitivity on inner surface of tube

The sensitivity analysis results were also compared with those obtained by finite difference method and good agreement was seen. Also, the accuracy of numerical evaluation of conditional variation was studied, and it was found that the normalized perturbation of a design parameter should be smaller than 10^{-7}. If a design parameter is significant in terms of sensitivity, larger perturbation may change the system state. It is therefore desirable that the perturbation should be prescribed as small as possible unless the round-off error occurs.

5. Conclusions

This work presented a sensitivity analysis method for treating frictionless contact problems with elasto-plasticity and large deformation. Sensitivity analysis algorithms based on the Lagrange multiplier and penalty contact constraint methods were formulated based on the direct differentiation method, where the conditional variation of contact force was numerically evaluated. This method can easily be implemented into an existing finite element analysis code. Consistent tangent stiffness for the contact problems was introduced and its necessity for sensitivity analysis was demonstrated via numerical examples. Use of approximated contact stiffness only affects the convergence of finite element analysis, though it may yield errors in the sensitivity analysis. Numerical examples demonstrated that the presented sensitivity analysis algorithm is effective from the aspects of accuracy and computational efficiency. Moreover, it was exemplified that, when applied to a real engineering problem, the sensitivity analysis results provide implications for design improvement and quality control. Future research will be directed at extending the present sensitivity analysis algorithm to handle frictional elasto-plastic contact problems.

References

[1] B. Cambou. Application of first-order uncertainty analysis in the finite element method in linear elastic. *Proc. of the 2nd International Conference on Applications of Statistics and Probability in Soil and Structural Engineering*, 87–97, 1975.

[2] X. Chen, T. Hisada, M. Kleiber, H. Noguchi. Comparison of different sensitivity analysis algorithms for large deformation elasto-plastic problems. In: M. Kleiber, T. Hisada, eds., *Design-Sensitivity Analysis*, 209–229, Atlanta Technology, 1993.

[3] X. Chen, T. Hisada, H. Noguchi, M. Mori. Nonlinear FEM-based sensitivity analysis of a grid spring in a nuclear fuel assembly (in Japanese). *Transactions of the Japan Society of Mechanical Engineers (A)*, **59**: 2742–2749, 1993.

[4] K. Dems, Z. Mroz. Variational approach by means of adjoint systems to structural optimization and sensitivity analysis – I. *Int. J. Solids Structures*, **19**: 677–692, 1983.

[5] K. Dems, Z. Mroz. Variational approach by means of adjoint systems to structural optimization and sensitivity analysis – II. *Int. J. Solids Structures*, **20**: 527–552, 1984.

[6] J.-H. Heegaard, A. Curnier. An augmented Lagrangian method for discrete large-slip contact problems. *Int. J. for Num. Meth. in Eng.*, **36**: 569–593, 1993.

[7] T. Hisada, S. Nakagiri. Stochastic finite element method developed for structural safety and reliability. *Proc. of the 3rd. International Conference on Structural Safety and Reliability*, 395–408, 1981.

[8] M. Kleiber. Shape and non-shape structural sensitivity analysis for problems with any material and kinematic non-linearity. *Comp. Meth. in Appl. Mech. and Eng.*, **108**: 73–97, 1993.

[9] M. Kleiber. Parameter sensitivity analysis in frictional contact problems of sheet metal forming. *Computational Mechanics*, **16**: 297–306, 1995.

[10] M. Kleiber, T.D. Hien. *The Stochastic Finite Element Method.* Wiley, Chichester, 1992.

[11] H. Parisch. A consistent tangent stiffness matrix for three-dimensional non-linear contact analysis. *Int. J. for Num. Meth. in Eng.*, **28**: 1803–1812, 1989.

[12] J.C. Simo, P. Wriggers, R.L. Taylor. A perturbed Lagrangian formulation for the finite element solution of contact problems. *Comp. Meth. in Appl. Mech. and Eng.*, **50**: 163–180, 1985.

[13] J.J. Tsay, J.S. Arora. Nonlinear structural design sensitivity analysis for path dependent problems. Part 1: General theory. *Comp. Meth. in Appl. Mech. and Eng.*, **81**: 183–208, 1990.

[14] J.J. Tsay, J.E.B. Cardoso, J.S. Arora. Nonlinear structural design sensitivity analysis for path dependent problems. Part 2: Analytical examples. *Comp. Meth. in Appl. Mech. and Eng.*, **81**: 209–228, 1990.

[15] Y. Zhang, A. Der Kiureghian. Dynamic response sensitivity of inelastic structures. *Comp. Meth. in Appl. Mech. and Eng.*, **108**: 23–36, 1993.

[16] Z.H. Zhong. *Finite Element Procedures for Contact-Impact Problems.* Oxford University Press, 1993.

[17] Z.H. Zhong, J. Mackerle. Static contact problems — a review. *Engineering Computations*, **9**: 3–37, 1992.

[18] O.C. Zienkiewicz, J.S. Campbell. Shape optimization and sequential linear programming. In: R.H. Galapher, O.C. Zienkiewicz, eds., *Optimum Structural Design*, 109–126. Wiley, 1989.